Contrib Mineral Petrol (2007) 154:575–590
DOI 10.1007/s00410-007-0210-z

ORIGINAL PAPER

Petrology and geochemistry of primitive lower oceanic crust from Pito Deep: implications for the accretion of the lower crust at the Southern East Pacific Rise

Neil W. Perk · Laurence A. Coogan · Jeffrey A. Karson · Emily M. Klein · Heather D. Hanna

Received: 25 September 2006 / Accepted: 13 April 2007 / Published online: 23 May 2007

Abstract A suite of samples collected from the uppermost part of the plutonic section of the oceanic crust formed at the southern East Pacific Rise and exposed at the Pito Deep has been examined. These rocks were sampled in situ by ROV and lie beneath a complete upper crustal section providing geological context. This is only the second area (after the Hess Deep) in which a substantial depth into the plutonic complex formed at the East Pacific Rise has been sampled in situ and reveals significant spatial heterogeneity in the plutonic complex. In contrast to the uppermost plutonic rocks at Hess Deep, the rocks studied here are generally primitive with olivine forsterite contents mainly between 85 and 88 and including many troctolites. The melt that the majority of the samples crystallized from was aggregated normal mid-ocean ridge basalt (MORB). Despite this high Mg# clinopyroxene is common despite model predictions that clinopyroxene should not reach the liquidus early during low-pressure crystallization of MORB. Stochastic modeling of melt crystallisation at various levels in the crust suggests that it is unlikely that a significant melt mass crystallized in the deeper crust (for example in sills) because this would lead to more evolved shallow level plutonic rocks. Similar to the upper plutonic section at Hess Deep, and in the Oman ophiolite, many samples show a steeply dipping, axis-parallel, magmatic fabric. This suggests that vertical magmatic flow is an important process in the upper part of the seismic low velocity zone beneath fast-spreading ridges. We suggest that both temporal and spatial (along-axis) variability in the magmatic and hydrothermal systems can explain the differences observed between the Hess Deep and Pito Deep plutonics.

Keywords Pito Deep · East Pacific Rise · Magma chamber · Mid-ocean ridge

Communicated by T. L. Grove.

Electronic supplementary material The online version of this article (doi:10.1007/s00410-007-0210-z) contains supplementary material, which is available to authorized users.

N. W. Perk · L. A. Coogan (✉)
School of Earth and Ocean Sciences, University of Victoria, Victoria, BC, Canada
e-mail: lacoogan@uvic.ca

J. A. Karson
Department of Earth Sciences, Syracuse University, Syracuse, NY 13244, USA

E. M. Klein
Nicholas School of the Environment, Duke University, Durham, NC, USA

H. D. Hanna
North Carolina Geological Survey, Raleigh, NC 27699, USA

Introduction

How the lower oceanic crust (i.e., the plutonic section) is accreted at fast-spreading ridges is unclear. Detailed geophysical studies at several locations in the oceans have provided snap-shots of the physical state of the lower crust. These studies have identified partially molten sills approximately 500–1,000 m wide and 10–50 m thick at, or near, the depth at which the transition from the sheeted dike to plutonic complex is predicted to occur (hereafter the axial magma chamber or AMC; e.g., Detrick et al. 1987; Kent et al. 1993). The AMC is underlain by a region of relatively low seismic velocities, that extends to the base of the crust, and which is interpreted to be a mixture of

crystals and melt (hereafter the low velocity zone or LVZ; Dunn et al. 2000; Crawford and Webb 2002). Two end-member models for the accretion of the lower oceanic crust basically differ in the proportion of the lower oceanic crust that crystallises in place within the LVZ versus crystallising in the AMC and subsiding to form the LVZ.

Models that suggest that most of the lower oceanic crust at fast-spreading ridges crystallizes in the AMC, and subsides to form the LVZ, are commonly referred to as ''gabbro glacier'' models (Fig. 1a). In this type of model primitive melt rises from the Moho to the AMC. Most crystal nucleation, and a substantial amount of crystal growth, occurs within the AMC and then a crystal mush subsides into the LVZ eventually solidifying to form new lower oceanic crust (Sleep 1975; Dewey and Kidd 1977; Nicolas et al. 1988; Quick and Denlinger 1993; Phipps-Morgan and Chen 1993; Henstock et al. 1993; Buck 2000). This model allows most of the latent heat of crystallisation of the plutonic rocks to be released in the AMC and extracted by the axial hydrothermal system. Replenishment, magma mixing and roof assimilation are expected to be important processes within the AMC in this scenario. This model is consistent with thermal constraints (e.g., Maclennan et al. 2004) and with the variation in seismic velocity with depth in the LVZ (Henstock et al. 2002). It is also consistent with the observation of strong crystal alignment, that occurred during melt-present flow, in gabbros from the Oman ophiolite (e.g., Nicolas et al. 1988; Quick and Denlinger 1993).

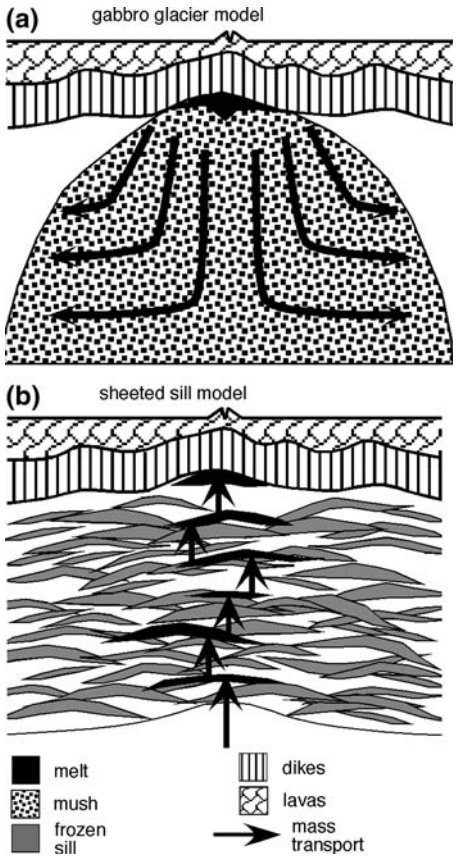

Fig. 1 End-member models for the formation of the lower oceanic crust at fast-spreading ridges: **a** a ''gabbro glacier'' model in which melt extracted from the mantle is delivered directly to the AMC where the majority of crystallisation occurs. The latent heat of crystallisation is removed by the axial hydrothermal system and the crystal mush that forms subsides to generate the lower crust (Quick and Denlinger 1993; Phipps Morgan and Chen 1993; Henstock et al. 1993; Buck 2000; Chen 2001; Henstock 2002); **b** a ''sheeted sill'' model (Reuber 1990; Bédard 1991; Kelemen et al. 1997; Kelemen and Aharanov 1998; Korenaga and Kelemen 1997, 1998; MacLeod and Yaouancq 2000; Garrido et al. 2001; Lissenberg et al. 2004) in which melt crystallises at all levels in the lower crust and the latent heat of crystallisation is released throughout the lower crust

The other end-member model suggests that most, or even all, of the lower crust crystallises in place, for example in sills, with nucleation and crystal growth occurring throughout the LVZ (Reuber 1990; Bèdard 1991; Kelemen et al. 1997; Kelemen and Aharanov 1998; Korenaga and Kelemen 1997, 1998; MacLeod and Yaouancq 2000; Garrido et al. 2001; Lissenberg et al. 2004). In this case the latent heat of crystallisation is released throughout the lower crust requiring deep hydrothermal circulation, and the AMC plays a smaller role in magma differentiation. Critically for this study, this model suggests that the upper plutonics crystallise from melts that have already precipitated cumulates in the deeper parts of the oceanic crust.

Hybrid models have also been proposed with significant amounts of crystallisation both in place in the LVZ and in the AMC (Boudier et al. 1996; Coogan et al. 2002a; Maclennan et al. 2004). In fact, the basic physics of both models require some proportion of each process. In the gabbro glacier model melt lubricates the subsiding crystal mush allowing it to flow; this melt is likely to crystallise in the deeper part of the crust. In the sheeted sill model the steeper thermal gradients, and thus more rapid cooling, at shallow than deep levels in the crust requires some crystal subsidence to prevent the AMC solidifying (e.g., Maclennan et al. 2004). This is accounted for in some (e.g., Kelemen et al. 1997; Kelemen and Aharanov 1998; Korenaga and Kelemen 1997, 1998) but not all (e.g., MacLeod and Yaouancq 2000; Lissenberg et al. 2004) sheeted sill models. Thus, the outstanding research questions involve the proportions of crystallization in different location and mechanisms of heat and mass transport within the lower crust.

One of the greatest difficulties with addressing these questions about lower crustal accretion at fast-spreading ridges is the paucity of samples from the lower oceanic crust that have been collected in situ. Only at Hess Deep have samples of more than just the upper ~100 m of the

gabbros been collected from sites where the spatial distribution of the samples is known. Here we present the results of a petrological and geochemical study of the upper ~900 m of the plutonic section of the lower oceanic crust formed at the East Pacific Rise (EPR) and exposed at Pito Deep. Although only approximately the upper quarter of the plutonic complex was sampled, these data place important constraints on the processes operating in the lower crust. The plutonic rocks recovered are mainly primitive (bulk-rock Mg# > 80) indicating that the melts that these rocks crystallized from had undergone little or no crystallisation at deeper levels. A stochastic model of melt crystallization in multiple sills is developed to predict the likelihood of the upper gabbros being primitive in this model.

Tectonic setting and previous work

Pito Deep is a bathymetric depression (~6,100 m) near a propagating rift tip at the northeastern corner of the Easter Microplate in the SE Pacific (Fig. 2). Nearby rift-bounding escarpments have >4,000 m of relief creating natural cross sections through the upper half of the oceanic crust that are tens of kilometers in length. The exposed crustal section initially formed at the fast-spreading southern EPR (>140 mm/year) about 3 Ma (Francheteau et al. 1988; Naar and Hey 1991; Searle et al. 1989; Martinez et al. 1991; Naar et al. 1991; Hey et al. 1995). This ''tectonic window'' into superfast-spread crust exposes continuous sections consisting of basaltic lavas, sheeted dikes, and gabbroic rocks (Constantin et al. 1995; Hékinian et al. 1996; Francheteau et al. 1988; Karson et al. 2005).

In the crust conjugate to that dismembered at Pito Deep, to the west of the EPR, lineated magnetic anomalies and abyssal hill fabrics are not interrupted by fracture zones or other discontinuities. Thus, the crust exposed at Pito Deep is thought to represent ''typical'' crust. Near Pito Deep, crustal blocks have been rotated 20°–30° clockwise about a vertical axis during the evolution of the Easter Microplate and rift propagation (Martinez et al. 1991; Naar et al. 1991; Hey et al. 1995). The main rift-bounding escarpments near Pito Deep cut the abyssal hill fabric at a very high angle, creating exposures with a nearly ideal orientation for observing spreading-related structures.

Plutonic rocks from the Pito Deep area were collected during two previous cruises. The SONNE 65 cruise (Stoffers et al. 1989; Constantin et al. 1995) recovered 16 gabbroic samples using a dredge while the Pito Nautile cruise (Hékinian et al. 1996) used the Nautile submersible to collect mostly dolerites as well as four gabbroic samples. Only two gabbroic samples collected in the above studies are known to come directly from outcrops. The plutonic rocks include gabbro, ferrogabbro, amphibolitised gabbro,

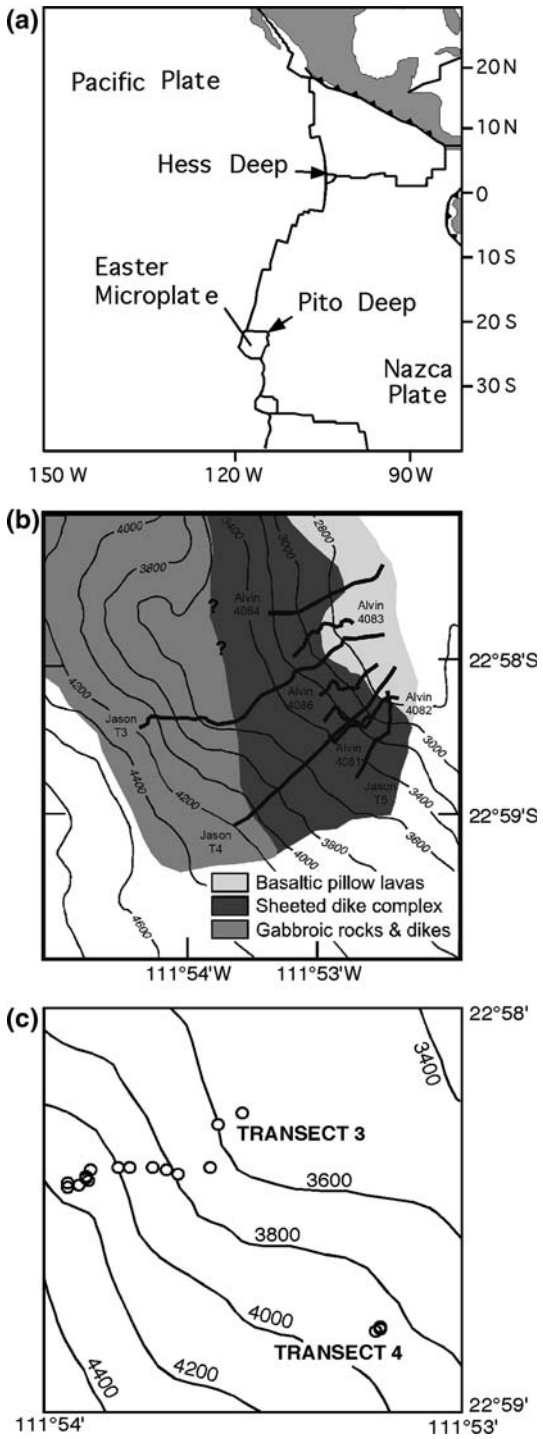

Fig. 2 Location and geological maps. **a** Map showing the Eastern Pacific region plate boundaries and the location of the Pito Deep and the Hess Deep—the only places where lower oceanic crust formed at fast-spreading ridge has been extensively sampled. Based on southward extrapolation of anomaly 2A from the north using the magnetic profiles of Naar and Hey (1991) and geomagnetic polarity timescales of Cande and Kent (1995) this crust is ~3 Myr old. **b** Geological map of the study area based on the Jason and Alvin dive program during cruise AT11-33 of the R/V *Atlantis* (dive tracks are shown as *black lines*; Karson 2005); **c** detail of the location of samples (*open circles*) discussed in this study

micro-gabbro, olivine gabbro, and leucotroctolite with primitive olivine gabbros being the most abundant rock type (Constantin et al. 1995, 1996; Hékinian et al. 1996).

Methods

Sample collection

During cruise AT11-33 of the R/V *Atlantis* (30 January to 8 March, 2005) two major escarpments were mapped and sampled with DSL-120 side-scan sonar, the submersible *Alvin*, and the remotely operated vehicle (ROV) *Jason II* (Karson et al. 2005). In this investigation, upper crustal basaltic lava and sheeted dike complex units cap an extensive outcrop area of gabbroic rocks. The internal structure (Morgan et al. 2005) and composition (Pollock et al. 2005; Heft et al. 2005) of these upper crustal units provide a framework for the consideration of the underlying gabbroic material.

In this area, the lavas and sheeted dikes together have a variable thickness (<1,500 m). The uppermost lavas, which include pillow, lobate and sheeted forms are only weakly fractured. Within the lava pile flow contacts can be seen to dip to the northwest; i.e., towards the EPR where the crust formed. Dikes in the lava sequence strike northeast and dip steeply to the southeast. This geometry persists downward into the sheeted dike complex. This general structure is similar to that found in other sections of fast-spread crust (Karson et al. 2002).

Samples of gabbroic rocks were collected in vertical sequences along two *Jason II* transects (Transect B3 and B4 of Morgan et al. 2005; Karson et al. 2005). Twenty-three samples of plutonic rocks were collected, twenty from Transect 3 and three from Transect 4. All of the samples were collected between 4,400 and 3,400 m below sea level, mainly from outcrops; a few samples come from talus. Samples recovered from talus are not believed to be far-traveled based on lack of evidence for large-scale mass wasting along the dive tracks. Both dives began in the plutonic complex and traversed upwards into the overlying sheeted dike complex allowing the sampling depth beneath the sheeted dike complex to be determined for all samples. For this study we estimate that the gabbro/sheeted dike contact is located at a depth halfway between the uppermost gabbro and lowermost dike samples. Using this datum, the gabbro samples come from 0 to 900 m below the sheeted dike complex (mbsd).

Samples of gabbroic rocks were collected by ROV with extensive video and digital still imagery with known geographic orientations. This permitted samples to be restored to approximate outcrop orientations by matching sample shapes and distinctive markings to in situ relations. This was essential to this study as textural details, such as layering or foliation, are obscured in seafloor outcrops by ferro-manganese coatings.

Analytical techniques

Bulk-rock compositions were determined on splits of each sample that had been trimmed of all visibly weathered surfaces and crushed in a steel mill. Bulk-rock major element analyses were determined at Duke University by direct current plasma emission sprectrometey (Fisons SpectraSpan 7) using methods modified after Klein et al. (1991). Bulk-rock trace element analyses were determined by inductively couled plasma mass spectrometry (ICP-MS) at The University of Victoria using a method based on that described by Eggins et al. (1997) using a Thermo X-series instrument (eTable 1). Certified reference materials were run as unknowns along with the samples and the results for these are also provided in eTable 1.

Major element compositions of plagioclase, olivine and clinopyroxene were determined by electron microprobe analysis at Leicester University using standard operating conditions (Coogan et al. 2000). Laser-ablation ICP-MS was used to analyse the cores of clinopyroxene crystals at the University of Victoria using NIST 611 to calibrate and Ca as the internal standard. There is little compositional zoning in any phase in either the major or trace elements analysed. Therefore the average composition of each phase was calculated based on ≥3 analyses (eTable 2).

Results

Petrography

The sample suite includes gabbros, olivine gabbros and troctolites along with one sample of diorite and one of anorthosite similar to the lithological variability described previously (Constantin et al. 1995, 1996). Accessory phases include Cr-spinel (in some troctolitic samples), orthopyroxene, apatite, amphibole, magnetite, ilmenite and sulphides. Plagioclase and olivine typically occur as granular crystals of varying grain size (<1 cm) while clinopyroxene is generally interstitial and forms oikocrysts (≤ 4 cm). The inclusion-free cores of clinopyroxene oikocrysts are ≤ 2 mm in size. The coarse grain size, and the uneven mineral distributions in many samples such as the occurrence of modal layering (Fig. 3a), means that modal mineralogy depends on the scale of measurement to some extent. Based on point counting, the troctolitic samples (<10% clinopyroxene) average 80% plagioclase and only 16% olivine generally similar to the leucotroctolites describe by Constantin et al. (1995). This is a higher pla-

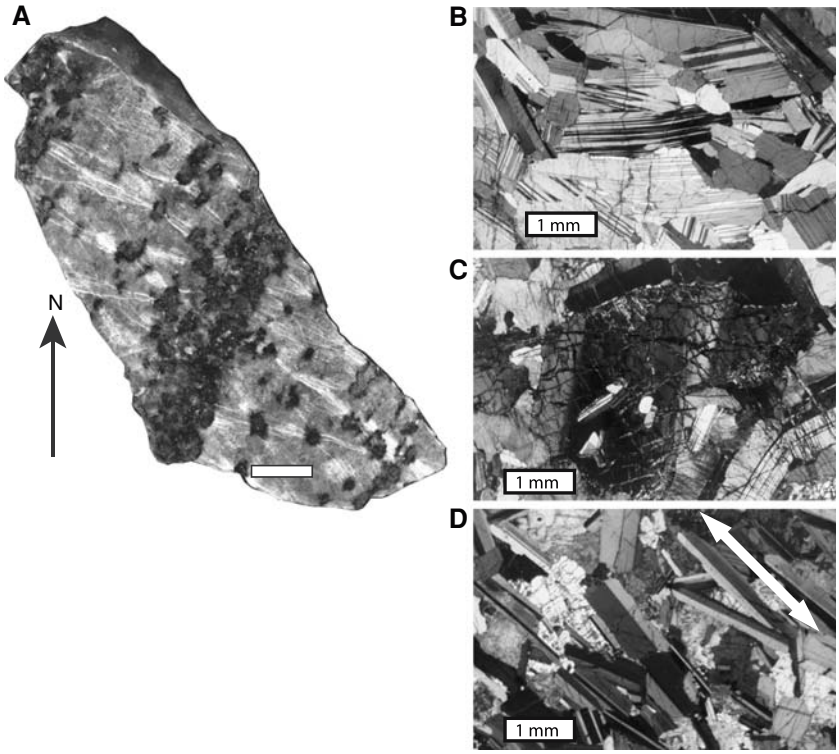

Fig. 3 **a** Photograph of a hand sample of layered troctolite (022005-0534) showing an olivine rich layer near the center of the sample. This is a top-down view of the sample with an approximate north arrow. The vertical modal layering is defined by an increase in the proportion of olivine in a ~3 cm thick layer parallel to the vertical foliation (striking ~ 020); **b** photomicrograph of a thin section of an anorthositic area of a troctolite (022005-0040) showing bent plagioclase containing tapering deformation twins typical of the most deformed samples; **c** photomicrograph of a thin section of an olivine gabbro (022005-0310) showing deformation bands in olivine typical of the most deformed samples; **d** photomicrograph of a thin section of an upper gabbro (022205-0230) showing a magmatic foliation defined by aligned plagioclase crystals (parallel to *white arrow*). Scale bar (*white rectangle*) = 2 cm in part (**a**) and 1 mm in parts (**b–d**)

gioclase-to-olivine ratio than that predicted for cotectic troctolite precipitation from MORB (mid-ocean ridge basalt) of ~70:30 (Grove et al. 1992). This may indicate preferential physical removal of olivine (e.g., by density segregation) presumably due to the existence of under-sampled olivine-rich layers.

The samples are generally fresh with only minor alteration (~5% secondary minerals), however, a few samples are highly altered ranging up to >95% replacement of primary igneous phases by hydrothermal minerals. Secondary minerals include amphibole, chlorite, talc and opaques.

Magmatic fabrics are common in this sample suite. These are typically defined by a preferred orientation of plagioclase crystals (Fig. 3d). Approximate reorientation of six samples to their orientation when sampled using multiple oriented video images shows that the in situ foliation is steeply dipping and currently strikes roughly N to NE; i.e., it is parallel to the regional seafloor spreading fabric and to the overlying dikes. Irrespective of the local extent of vertical-axis rotation, the foliation was originally approximately ridge parallel and sub-vertical, similar to the foliations that occur in the upper gabbros at Hess Deep (Gillis et al. 1993; MacLeod et al. 1996) and in the Oman ophiolite (e.g., Boudier et al. 1996).

A notable feature of the gabbroic rocks from the Pito Deep is the presence of minor crystal-plastic deformation in nearly all samples collected from >100 mbsd. This is manifest as bending and tapering of plagioclase twins as well as undulose extinction and sub-grains in olivine (Fig. 3b, c). A qualitative analysis of the extent of crystal-plastic deformation, based on the distribution of these features, suggests an increase in the extent of crystal plastic deformation with depth below the sheeted dike complex. Evidence for crystal-plastic deformation has not previously been reported for plutonic rocks formed at the EPR to our knowledge except those intruding peridotites within transform faults (Constantin 1999).

Geochemistry

Whole rock geochemistry

The bulk-rock composition of plutonic rocks from the study area (Fig. 2) are mainly at the primitive end of the

global spectrum of oceanic plutonic rocks with high Mg#'s (Mg# = 100 × Mg/(Mg + Fe); in cation proportions) and low concentrations of incompatible elements (e.g., TiO_2; Fig. 4a). The observation that they are largely troctolitic (eTable 2) is consistent with the Mg–Al systematics that are simply explained by a mixture of plagioclase and olivine for the majority of samples (Fig. 4b). A smaller number of samples are gabbroic and these overlap the main field of plutonic rock analyses from the modern ocean basins (Fig. 4b). Despite being primitive in terms of Mg# the troctolites are generally not extremely MgO-rich (average 11 wt.% MgO) due to the high proportion of plagioclase in these rocks.

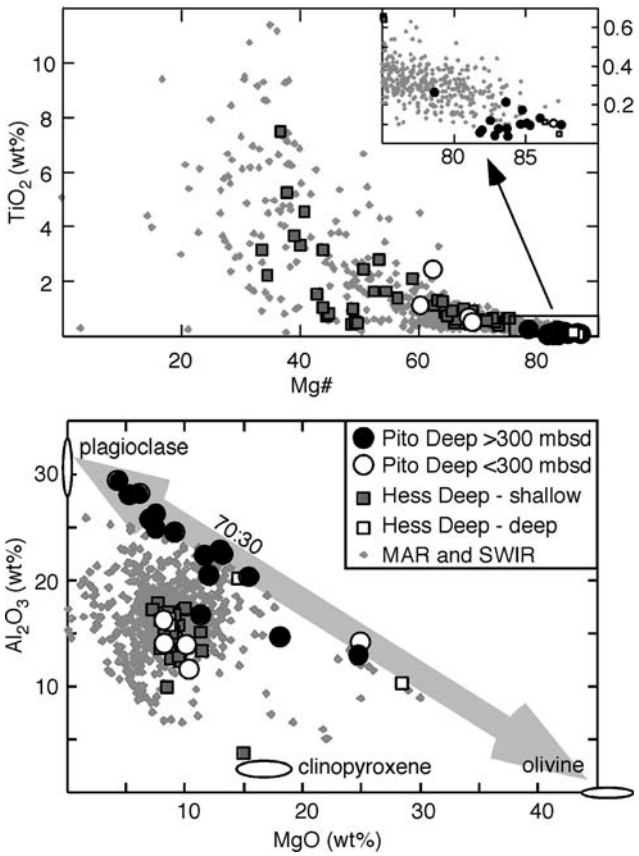

Fig. 4 Bulk-rock major element systematics of Pito Deep plutonic rocks: (**a**) Mg# versus TiO_2 demonstrating that most of the Pito Deep rocks lie at the most primitive end of the global spectrum with high Mg#'s and low TiO_2 contents; (**b**) Bulk-rock MgO versus Al_2O_3 (wt%) showing that the Pito Deep rocks are largely troctolitic lying on a mixing line between olivine and plagioclase. Only five samples fall within the main field of gabbro compositions from other areas in the modern ocean basins. Upper gabbros from Hess Deep have gabbroic compositions similar to the majority of oceanic gabbros. MAR = Mid-Atlantic Ridge; SWIR = Southwest Indian Ridge (based on data compilations in Coogan 2007). Ovals labeled olivine and plagioclase show the compositions of these phases in the clinopyroxene-poor samples

The samples studied are light rare earth element (LREE) depleted with positive Sr and Eu anomalies (Fig. 5). These positive anomalies are typical of plutonic rocks from the oceanic crust (e.g., Pedersen et al. 1996) due to the accumulation of plagioclase. The lack of a positive Ti anomaly in most samples indicates that their parental melts were not saturated in FeTi oxides. A single, relatively evolved, sample from 253 mbsd on Transect 3 does have a positive Ti anomaly. This sample also has a high Ti content for its Mg# (Fig. 4a) compared to the rest of the samples indicating that it contains cumulus FeTi oxides. This is consistent with the occurrence of several percent ilmenite in its mode (along with amphibole, apatite, titanite and quartz all of which are interpreted to be magmatic). The samples studied generally have much lower abundances of highly incompatible trace elements than basalts from the overlying upper crust (e.g., on average ten-fold lower REE abundances; Fig. 5). This indicates that they are cumulates rather than frozen liquids—a point returned to below.

Before using the bulk-rock trace element compositions of plutonic rocks to investigate their parental melt compositions, compositional differences resulting from variations in modal proportions must first be evaluated. For example, bulk rock REE trends will depend on the relative mineral proportions, especially the proportions of plagioclase and clinopyroxene, as these minerals partition the REEs very differently. Plagioclase has higher partition coefficients for the LREE's than heavy REE's (HREE's) while the opposite is true of clinopyroxene. Plagioclase is also highly enriched in Eu over the other REE's; thus the Eu/Eu* ratio provides a rough guide to the amount of plagioclase accumulated in a sample (Eu/Eu* correlates with both the modal proportion of plagioclase determined

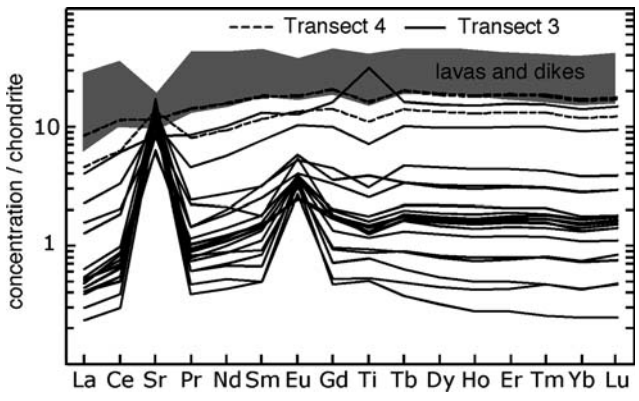

Fig. 5 C1 chondrite normalised (Anders and Grevesse 1989) bulk-rock spider diagram. Note the large positive Sr and Eu anomalies indicating plagioclase accumulation and the generally low REE element abundances. The grey field shows the composition of lavas and dikes collected on the same cruise as the plutonic rocks from the overlying upper crust (Pollack et al. 2005; Pollack et al., unpublished data)

from point counting and with the bulk-rock Al_2O_3 content). The effects of these different partition coefficients can be seen in Fig. 6. Samples with higher plagioclase/clinopyroxene ratios have higher Eu/Eu* and higher La/Sm than those with lower plagioclase/clinopyroxene ratios. A general mixing trend between plagioclase-rich and clinopyroxene-rich samples can be seen in the REE data but four samples stand out from this trend (Fig. 6).

Three samples from Transect 4, ~1 km to the South-East of Transect 3, have higher La/Sm for a given extent of plagioclase accumulation (shown by Eu/Eu*; Fig. 6)—this is also observed in the REE composition of clinopyroxene as discussed in the following section. This LREE-enrichment can either be explained by crystallization from a LREE-enriched parental melt, or by reaction with a large amount of interstitial melt. In the latter scenario the bulk-rock REE ratio in the gabbro are almost identical to those of the melt. The fourth sample (022005-0241) is from Transect 3. This sample also has an anomalously high La (and Ba) concentrations for a given Mg#, the lowest Cu concentration (5 ppm) of all the samples, and is extensively altered with nearly complete replacement of mafic phases—amphibole being the most abundant secondary mineral. Based on this we hypothesise that the LREE-enrichment in this sample may be related to hydrothermal alteration.

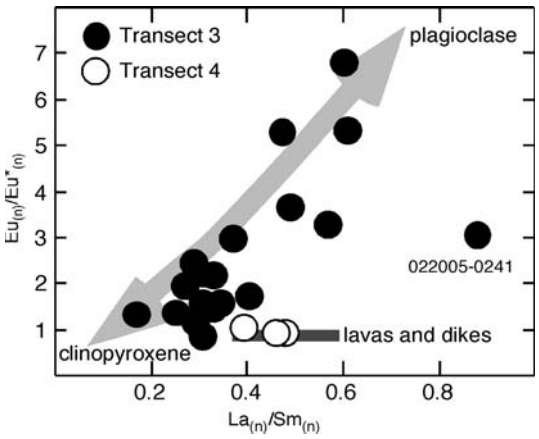

Fig. 6 Bulk rock C1 chondrite normalised La/Sm vs. Eu/Eu* (Eu* = [Sm + Gd]/2). Samples from Transect 3 define a mixing trend between plagioclase (high La/Sm and high Eu/Eu*) and clinopyroxene (low La/Sm and low Eu/Eu*) based on the relative partitioning of these elements measured in gabbros from the Oman ophiolite (Kelemen et al. 1997). Samples from Transect 4 all have high La/Sm for a given Eu/Eu* suggesting that they either crystallised from a parental melt with higher La/Sm than the parental melt for samples from Transect 3 or contain a higher proportion of trapped melt. The grey box shows the composition of 97% of the lavas and dikes collected on the same cruise as the plutonic rocks from the overlying upper crust (Pollack et al. 2005; Pollack et al., unpublished data)

Mineral Chemistry

Previous studies of plutonic rocks from the Pito Deep found two relatively homogenous but largely distinct groups (Constantin et al. 1995, 1996). Constantin et al. (1996) report troctolitic rocks containing plagioclase (An_{80-86}), olivine (Fo_{85-88}) and minor clinopyroxene ($Mg\#_{86-91}$) and (olivine-) gabbros containing plagioclase (An_{58-74}), olivine (Fo_{72-77}) and clinopyroxene ($Mg\#_{74-83}$). In this study, we found that below a depth of 300 mbsd, the major element compositions of plagioclase (An_{77-85} with the exception of one sample with An_{70}), olivine (Fo_{83-88}) and clinopyroxene ($Mg\#_{85-89}$) are relatively homogenous and primitive (Figs. 7, 8). Compatible minor elements are also relatively high in both clinopyroxene (Cr_2O_3 = 0.04 – 1.24 wt.%) and olivine (NiO = 0.10 to 0.21 wt.%) at depths >300 mbsd. The upper 300 m of the plutonic

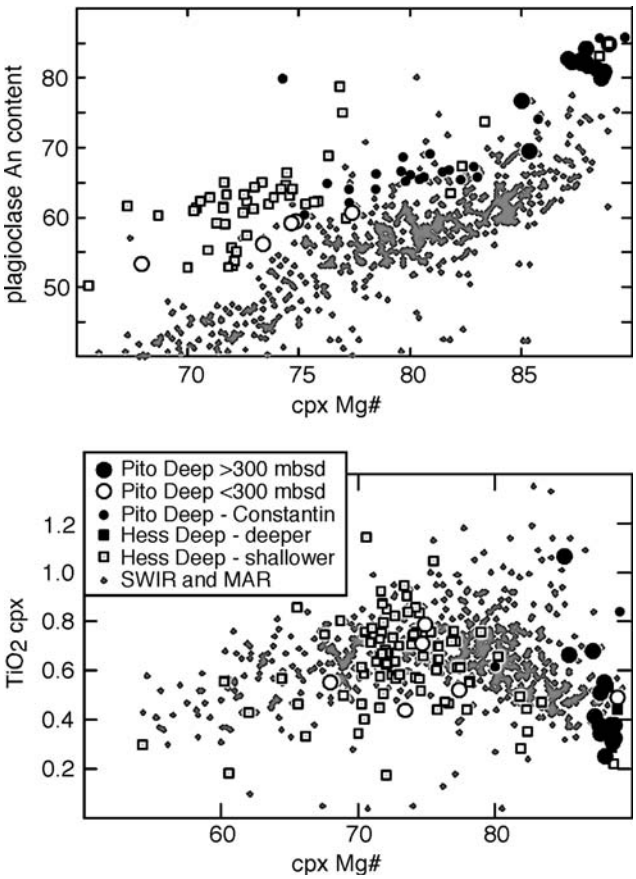

Fig. 7 Mineral major element chemistry: **a** clinopyroxene Mg# versus coexisting plagioclase anorthite content; **b** clinopyroxene Mg# versus TiO_2 content. Note that the Pito Deep samples collected from >300 mbsd fall at the most primitive end of the global spectrum. The broad difference between the trends in part (**a**) reflect differences in the Na content of the parental magma (e.g., Fig. 10a in Coogan 2007). MAR = Mid-Atlantic Ridge; SWIR = Southwest Indian Ridge (based on data compilations in Coogan 2007)

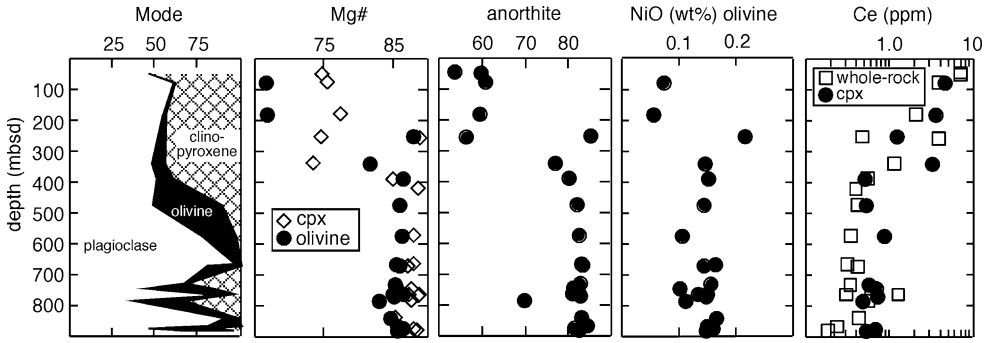

Fig. 8 Modal and compositional variation with depth beneath the sheeted dike complex (mbsd) for both dive tracks combined: **a** mineral modes as determined by point counting; **b** Mg# of olivine and clinopyroxene; **c** an content of plagioclase; **d** NiO in olivine; and **e** Ce in both bulk-rocks and clinopyroxene. Note that beneath ~300 mbsd the rocks are uniformly primitive with low incompatible trace element abundances and high compatible trace element abundances

section is more evolved and shows more compositional variation than the deeper samples ($Fo_{66\text{-}77}$, $An_{56\text{-}70}$, clinopyroxene $Mg\#_{68\text{-}77}$).

Clinopyroxene generally has a LREE-depleted pattern similar to clinopyroxene from other plutonic rocks from the modern ocean basins (Fig. 9). Clinopyroxene REE abundances generally range from 1 to 2 times C1 chondrite for Ce and 4–9 times C1 chondrite for HREE for samples collected from >350 mbsd. Closer to the base of the sheeted dike complex clinopyroxene REE abundances are higher at 5–8 times C1 chondrite for LREE and 17–40 times C1 chondrite for HREE (Fig. 9). Most clinopyroxene crystals are depleted in Eu relative to the adjacent REE's and this anomaly becomes larger with increasing REE concentrations. This feature is observed in clinopyroxene from other oceanic gabbros and indicates co-precipitation of plagioclase (e.g., Coogan 2007). This cannot be explain by subsolidus exchange of Eu with adjacent plagioclase because there is no obvious reason why this would only occur more in the samples with more REE-rich clinopyroxene. The only sample from Transect 4 analyzed for clinopyroxene trace elements is LREE-enriched compare to all other clinopyroxene analysed (Fig. 9). For example, clinopyroxene in this sample has $Ce_{(n)}/Yb_{(n)} = 0.42$ but all clinopyroxene crystals from Transect 3 that were analysed have $0.1 < Ce_{(n)}/Yb_{(n)} < 0.2$. Two models can explain this: either (1) this sample crystallised from a melt with a Ce/Yb ratio approximately twice as high as that of the melt that the Transect 3 gabbros crystallised from; or (2) this sample is compositionally a frozen liquid rather than a cumulate. With the current data it is not possible to unambiguously distinguish between these alternative models.

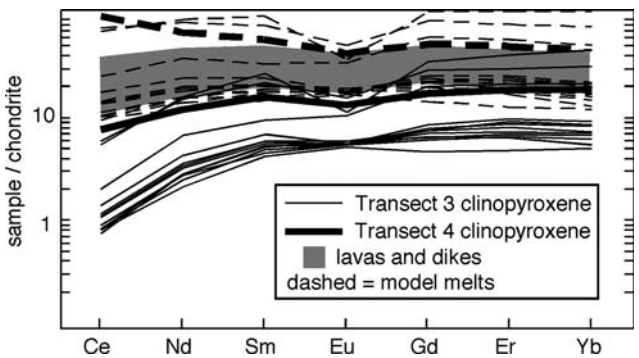

Fig. 9 C1 chondrite normalised (Anders and Grevesse 1989) REE spider diagram showing clinopyroxene compositions and the compositions of melts calculated to be in equilibrium with these. Melt compositions were calculated using the partition coefficients of Hart and Dunn (1993) except for Gd which was interpolated from the neighboring REE's. The *grey field* shows the composition of lavas and dikes collected on the same cruise as the plutonic rocks from the overlying upper crust (Pollack et al. 2005; Pollack et al., unpublished data)

Modelling crystallisation of the Pito Deep plutonic rocks

Parental melt composition

Parental melt REE contents and Mg#'s have been calculated based on the clinopyroxene and olivine compositions. These were calculated using an olivine Mg–Fe partition coefficient ($K_D^{Fe-Mg} = \{[X_{Fe}^{xtal}][X_{Mg}^{xtal}]\}/\{[X_{Fe}^{liq}][X_{Mg}^{liq}]\}$) of 0.29 (Grove et al. 1992), a clinopyroxene K_D^{Fe-Mg} of 0.23 (Grove and Bryan 1983; Tormey et al. 1987) and REE distribution coefficients (k_d) from Hart and Dunn (1993). All samples collected at >300 mbsd are in equilibrium with a melt with 10–30 times C1 chondrite REE abundances and $Mg\#_{57\text{-}65}$. These compositions are similar to those of the more primitive lavas sampled from the overlying lavas and dikes (Hékinian 1996; Pollock et al. 2005) indicating that the melts that the plutonic rocks crystallised from were aggregated MORB. The more evolved samples, recovered

from the upper 300 m of the plutonic section, are not in REE, or Mg–Fe, equilibrium with erupted MORB from Pito Deep.

''Trapped melt'' contents

The bulk-rock composition of plutonic rocks is determined by not just the composition of the parental melt and the modal proportion of cumulus crystals but also the amount that cumulus crystals react with interstitial melt after initial crystal accumulation. This process is commonly referred to, and modeled as, a trapped melt shift in which the bulk rock composition is assumed to be made up of the cumulus crystals plus some portion of trapped parental melt. This is somewhat misleading because interstitial melt is very unlikely to be stationary and instead will migrate through the crystal mush reacting with it. However, trapped melt fractions (TMF), if calculated appropriately, will generally provide an upper bound on the amount of truly trapped melt and provide a tool to compare the extent of reaction between interstitial melt and cumulus crystals in different plutonic suites. We stress that these are not masses of melt that physically became trapped in the rock. Instead the TMF is a proxy for the volume of parental melt that would have to have been trapped to change the bulk composition of a perfect cumulate to the observed bulk composition. This may occur in differing ways; for example, reaction of the cumulus crystals and interstitial melt may occur and/or overgrowth of the cumulus crystals and growth of additional interstitial phases can happen.

Fictive TMF's were calculated as follows. Clinopyroxene core compositions and published inter-mineral partition coefficient (here taken from Bédard 1994) were used to calculate the composition of cumulus plagioclase and olivine. This assumes that the compositions of clinopyroxene crystal cores have not been modified after they initially grew which is consistent with the very slow diffusion of REE's in clinopyroxene (Van Orman et al. 2001). The bulk composition of a perfect cumulate (X_x) can then be calculated from the sum of the modal fraction (F) of each phase and its measured (clinopyroxene) or calculated (plagioclase and olivine) composition ($X_{mineral}$):

$$X_x = F_c \cdot X_c + F_p \cdot X_p + F_o \cdot X_o \quad (1)$$

where c = clinopyroxene, p = plagioclase and o = olivine.

The difference between the calculated composition of the perfect cumulate and the measured bulk composition is then assumed to be due to reaction with interstitial melt. The bulk composition of a rock (X_B) is the sum of the composition of the crystals (X_X) and the composition of the trapped melt (X_{TM}) multiplied by their proportions.

$$X_B = (F_X \cdot X_X) + (F_{TM} \cdot X_{TM}) \quad (2)$$

where F_X is the fraction of cumulus crystals and F_{TM} is the fraction of trapped melt and $F_X = 1 - F_{TM}$. Assuming that the clinopyroxene crystal cores were in equilibrium with the trapped melt, then $X_{TM} = X_c/k_d$ which can be calculated using the measured clinopyroxene composition and the relevant clinopyroxene partition coefficient. Making these two substitutions:

$$X_B = ([1 - F_{TM}] \cdot X_X) + (F_{TM} \cdot [X_c/k_d]) \quad (3)$$

And isolating F_{TM}:

$$F_{TM} = (X_B - X_X)/((X_{cpx}/k_d) - X_X) \quad (4)$$

This allows the TMF (F_{TM}) to be calculated based on the measured bulk rock and clinopyroxene compositions, modal proportions and partition coefficients for clinopyroxene, plagioclase, and olivine. Using this approach for the nine samples for which all necessary data are available yields TMF's of <0.05 based on four different REE's that we have clinopyroxene and bulk rock analyses of (Ce, Sm, Gd, Er).

High Mg# clinopyroxene crystallised at low pressure

All samples studied here were collected <1 km below the base of the sheeted dike complex. At this depth beneath the ridge axis seismic studies suggest that the crust is partially molten (e.g., Dunn et al. 2000). This suggests that these samples solidified at their sampling depth and were not brought up from deeper levels after solidification. Even if some crystallisation occurred at greater depths, with these crystals transported upwards by magmatic flow, they would be likely to re-equilibrate to the new pressure-temperature conditions in the shallow crust before solidification.

If these arguments that the sample suite equilibrated at low pressure are correct this shallow level crystallisation raise a question regarding the origin of the high Mg#s in clinopyroxene (Mg#'s of 87–89 in thirteen samples; Figs. 7, 8). Experimental studies suggest that the first clinopyroxene to crystallise from primitive basaltic melts at low pressure will have an Mg# of ~84 (Grove and Bryan 1983; Tormey et al. 1987; Grove et al. 1992). At higher pressures clinopyroxene reaches the liquidus after smaller amounts of olivine and plagioclase crystallisation and hence the first clinopyroxene to crystallise has a higher Mg#. This experimental evidence for late clinopyroxene crystallisation on the MORB liquid line of decent at low pressure has been used to argue that high-Mg# clinopyroxene in oceanic gabbros from slow-spreading ridges provide evidence for high-pressure crystallisation (e.g.,

Elthon et al. 1992). Additionally, evidence for early clinopyroxene crystallisation, based on differentiation trends in MORB, has been used as evidence for high-pressure crystallisation of basalts at slow spreading ridges (e.g., Tormey et al. 1987; Grove et al. 1992; Meyer and Bryan 1996; Herzberg 2004). Assuming that the high Mg# clinopyroxene in the Pito Deep plutonics did not crystallise at high pressures their occurrence raises significant doubts about these interpretations. At least three models for the high Mg# clinopyroxene at Pito Deep can be envisaged:

1. Accumulated olivine may have buffered the Mg# of interstitial melt from which clinopyroxene crystallised. Clinopyroxene could grow from the interstitial melt in a troctolitic cumulate, with its Mg# buffered by the high abundance of magnesian olivine. This model can readily explain the high Mg# of clinopyroxene samples with high modal proportions of olivine and only minor clinopyroxene. However, other samples, such as 022005-0910 contains 40% clinopyroxene (Mg# 88.6) and only 10% olivine (modal proportions from thin section point counting). If the same model is to explain the Mg# of the olivine in this sample then the interstitial melt must have been buffered by olivine at least cm away from the growing clinopyroxene.
   Because the clinopyroxene oikocrysts are compositionally homogeneous and these rocks have low ''trapped melt fractions'', the interstitial melt from which these rocks crystallised must have been continually extracted from the crystal mush during clinopyroxene crystallisation. If this was not the case the trapped melt fraction would have to be ~2.5 times greater than the modal proportion of clinopyroxene (based on crystallization at cotectic proportions) and the clinopyroxene oikocrysts would be strongly zoned which they are not. Thus, even if the high Mg# of many clinopyroxene is due to melt-olivine reaction buffering the interstitial melt composition the interstitial melt that was co-saturated with olivine, plagioclase and clinopyroxene at low pressure may have been returned to an eruptible magma reservoir. Mixing this melt back into an eruptible reservoir (i.e., in situ crystallisation; Langmuir 1989) would imprint a geochemical signature of early clinopyroxene crystallisation even through low-pressure crystallisation.

2. The melts parental to the high Mg# clinopyroxene may not have been fully aggregated MORB (i.e. different melt fractions produced in the mantle may not have fully mixed together prior to crystallization starting; e.g., Grove et al. 1992). For example, they may have had high Ca/Al leading to an increase in the stability of clinopyroxene with respect to plagioclase (e.g., Coogan et al. 2000). However, this model seems unlikely because trace element evidence suggests a fully aggregated parental melt (see ''Parental melt compositions'').
3. Experimental studies may not replicate natural phase equilibria perfectly. For example, slow clinopyroxene nucleation in experiments may prevent its crystallisation even when it is thermodynamically stable. Alternatively, higher chromium and/or water contents in primitive MORB than in the starting materials used in experimental studies may enhance clinopyroxene stability.

Regardless of its origin, the occurrence of high Mg# clinopyroxene in the Pito Deep gabbros suggests that this is not a good indicator of high-pressure crystallisation. Thus, neither high Mg# clinopyroxene in ocean gabbros, nor evidence of early clinopyroxene crystallisation in MORB differentiation trends, provide firm evidence for high-pressure crystallisation. The alternative model, that the samples studied crystallised at high-pressure and were subsequently transported large distances vertically in the solid-state, is difficult to reconcile with geophysical data from, and thermal models of, fast-spreading ridges.

Modelling compositional variation with depth in the crust

The presence of primitive cumulates in the upper 1,000 m of the lower oceanic crust at Pito Deep provides evidence that mantle-derived melts can be transported to shallow levels with minimal differentiation occurring en-route. The fact that these are primitive, rather than evolved gabbros, suggests that they did not crystallise from melts that had migrated from the Moho to the AMC precipitating the deeper gabbros en route (e.g., Fig. 1b). Instead, it is likely that the parental melts were transported directly from the Moho into the upper crust (e.g., Fig. 1a). If they did pool in multiple sills in the deeper crust (e.g., Fig. 1b) then they did not crystallise much mass in these sills and thus they did not contribute significantly to lower crustal accretion through crystallisation in sills. Likewise, they did not release much of their latent heat of crystallisation in the deeper portion of the plutonic section of the crust. The same observation of primitive upper gabbros that cannot have crystallised much mass in the deeper crust has been made for the Oman ophiolite (Coogan et al. 2002c). Primitive high-level gabbros suggest either that: (1) all melts are added directly to the AMC and the deeper gabbros form from cumulates subsiding from this body (Fig. 1a), or (2) melts only pond in a single sill within the lower crust with any residual melt extracted directly into the lavas and dikes. In either case

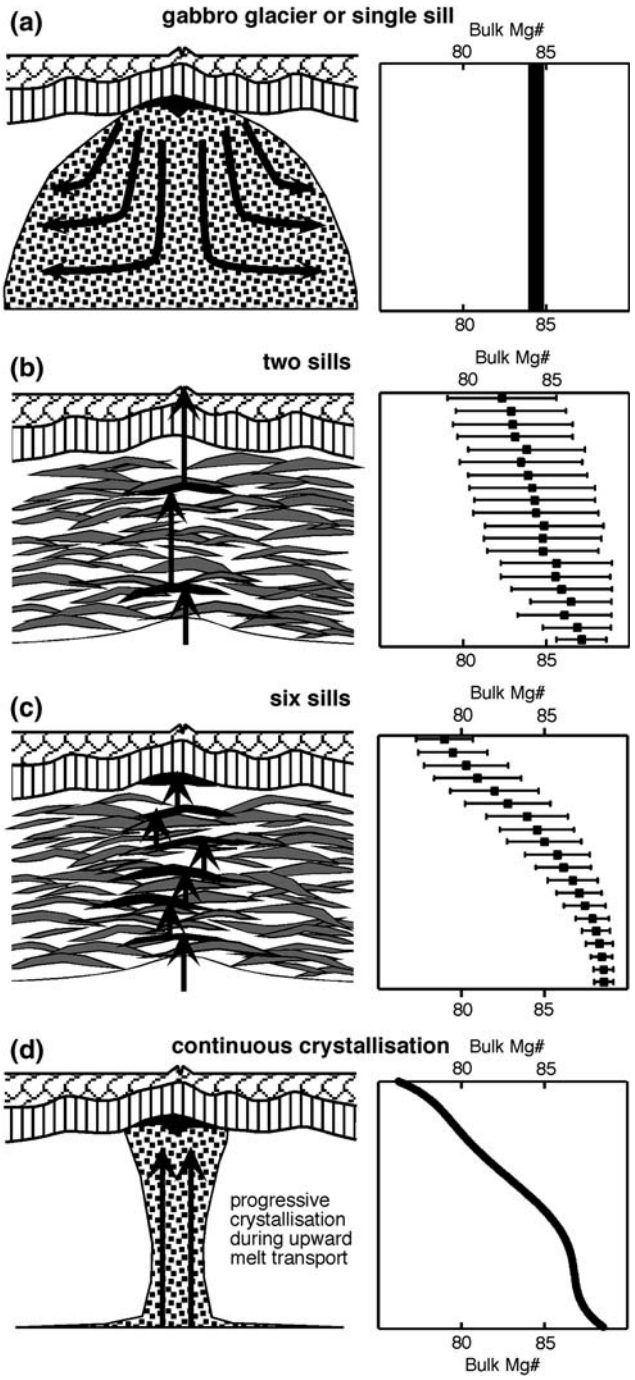

◀ **Fig. 10** Modeled variation in average bulk-rock composition versus depth in the lower crust for different styles of lower crustal accretion: **a** in the gabbro glacier model the average composition of the lower crust is constant with depth. This is also true for a sheeted sill model in which melts only pond in one sill in the lower crust; **b** if melts pond in two sills then, although the average composition gets more evolved with height in the crust there is still a high probability that primitive cumulates will form at shallow crust levels; **c** if melts pond in six sills in the lower crust then there is a low probability of primitive cumulates forming at shallow levels in the plutonic section; and **d** if melts pond in an infinite number of sills, or melts crystallise along the margins of a dike, then the composition of the lower crust would become systematically more evolved upwards with no heterogeneity. Shading as in Fig. 1. The *horizontal bars* show the standard deviation of the composition of cumulates formed at any given depth in the model; note the larger range of composition predicted at any given depth by the two-sill model than by the six sill model

there should be little systematic variation in large-scale crustal composition with depth. Alternatively, if melts pond in multiple sills the lower crustal composition should become more evolved upwards.

To investigate this argument quantitatively we have performed a series of stochastic models of melt ponding in multiple sills within the crust to predict how the bulk composition of the crust will change with height dependent on the number of sills that melt ponds, and crystallise, within. We use this approach because both the depth of sill emplacement and the fraction of crystallisation in each sill are not predicted by current models. We performed a series of Monte Carlo simulations of this process as follows (see eAppendix for more details):

1. The bulk composition of a cumulate (zero trapped melt) generated during any crystallisation interval was parameterised as a function of the proportion of melt remaining assuming perfect fractional crystallisation. This was modelled using the MELTS algorithm (Ghiorso and Sack 1995) using the average of the primitive MORB compilation of Presnall and Hoover (1987) as a starting composition.
2. To simulate a single melt batch being transported through the crust and ponding and partially crystallizing in multiple sills we use a stochastic model. Both the extent of crystallisation in each sill, and the depth of injection of each sill, are randomly generated. However, for any given magma batch each sill is emplaced at a shallower depth than the previous one. The melt fraction crystallized in each sill is normalised to sum to 0.7 for all sills based on the assumption that 70% of the crust is plutonic rocks and 30% is dikes and lavas; i.e. each magma batch is forced to crystallize 70% within the plutonic crust but this is divided randomly between the different sills it ponds in. The depth of sill emplacement is normalized to sum to the thickness of the plutonic complex. This procedure is repeated 10,000 times for each model run.

If melts are all added directly to the AMC and cumulates subside as in the ‘‘gabbro glacier’’ model the average lower crust gabbro has an Mg# of 84. There will be random fluctuations around this dependent on variations in the extent of crystallisation in the AMC prior to eruption and post-cumulus processes (Fig. 10a). Likewise, if melts pond in a single sill, and crystallise in place, then the average crustal composition will be the same and there will also be

random variations in composition dependent on the extent of crystallisation that may vary between sills. In either of these cases there will be no systematic variation in the bulk composition of the plutonic section with depth in the crust.

In contrast to the gabbro glacier and single sill scenarios, if melts pond and crystallise in multiple sills then the bulk lower crustal composition must become more evolved upwards. If melts pond only in two sills then there is a high probability that both sills will be at shallow levels in the crust. This leads to there being a high probability of primitive cumulates forming at shallow levels. This means that the average composition of the upper plutonic rocks is only slightly more evolved than that of the lower plutonic rocks; additionally the standard deviation about the average composition in the upper portion of the plutonic complex is large.

As the number of sills that a magma ponds in becomes greater the variation in composition towards more evolved plutonic rocks at shallow levels becomes more systematic (Fig. 10c). This is because the probability of primitive melts traveling through the deeper crust without fractionating is small although non-zero. Likewise, the chance of a melt becoming highly fractionated in the lower crust is small. In the six-sill model the average composition in the plutonic complex becomes systematically more evolved upwards and the standard deviation about this average is much smaller than in the two-sill model. If melts crystallise continuously as they traverse through the crust, either in an infinite number of sills, or on the ''walls'' of a dike-like melt transport channel, then the composition of the lower crust will become systematically more evolved upwards (Fig. 10d).

The simple modelling shown in Fig. 10 suggests that in areas where the upper gabbros are composed almost entirely of primitive cumulates, such as at Pito Deep, the crust is unlikely to be constructed as a series of sheeted sills with melts ponding in numerous sills within the crust. The result could be more ambiguous if the crystallisation process varies (e.g., fractional to equilibrium), if there are variations in the fraction of ''trapped melt'', or if the crystallisation and ponding processes are not random. Equilibrium rather than fractional crystallisation will tend to damp the compositional variability observed but will not change the overall patterns. Variations in cooling rate are likely to lead to greater extents of trapped melt in the faster cooling shallow gabbros because compaction will be less efficient at removing the interstitial melt out of the mush. Because of this, the occurrence of evolved upper gabbros may not require a multiple-sills mechanism of crustal accretion. In contrast, the occurrence of primitive upper gabbros does argue against melts ponding and crystallizing a substantial mass in multiple sills within the lower crust.

In summary, it seems clear that at Pito Deep the lower crust was not constructed through crystallisation in multiple sills emplaced at different levels in the lower crust. If melts only pond in a single sill within the lower crust then we would expect the seismically determined depth to the AMC (a magma sill) to be highly variable, occurring at all levels in the LVZ, which it is not. Furthermore, the sheeted dike to gabbro transition should be gradual with dikes occurring throughout the plutonic complex which is not generally observed either in tectonic windows such as Pito and Hess Deep or in the Oman ophiolite.

Comparison to Hess Deep and implications for lower crustal heterogeneity along the EPR

Hess Deep (Fig. 2) is the only other location where samples from more than the upper 100 m of the lower oceanic crust formed at a modern fast-spreading ridge have been recovered. Similar magmatic foliations are seen in Pito Deep plutonic rocks as those described in samples from Hess Deep (e.g., Gillis et al. 1993; MacLeod et al. 1996) and in the Oman ophiolite (e.g., Boudier et al. 1996). Assuming that these fabrics form through crystal alignment during flow of a crystal mush (Nicolas 1992), this suggests that near-vertical and axis-parallel magmatic flow is common in the upper part of the LVZ at fast-spreading ridges. Unlike gabbros from Hess Deep, which show very little evidence for crystal plastic deformation (e.g., MacLeod et al. 1996; Coogan et al. 2002a), most samples from Pito Deep do show some evidence of crystal plastic deformation (Fig. 3b, c). The presence of crystal plastic deformation in the upper plutonic section at Pito Deep suggests that they were subject to more, although still minor, high-temperature strain than rocks from the same structural level at Hess Deep.

In contrast to the similarity in the foliation in the Hess Deep and Pito Deep plutonic suites, compositionally they are strikingly different. The plutonic rocks at Pito Deep are much more primitive than those from a similar structural level at Hess Deep (i.e. the upper part of the north scarp and the upper part of the intra-rift ridge; Hékinian et al. 1993; Gillis et al. 1993; Natland and Dick 1996; Pedersen et al. 1996; Hanna 2004; Coogan et al. 2002a). At Hess Deep, evolved gabbronorites are common and troctolites, anorthosites and Cr-spinel bearing samples are rare and have only been recovered from deeper levels on the intra-rift ridge (Hékinian et al. 1993). In contrast, at Pito Deep orthopyroxene is rare and Cr-spinel bearing troctolites are abundant in the upper plutonic rocks. Nearly all samples from >300 mbsd at Pito Deep have more primitive compositions than samples from equivalent depths beneath the sheeted dike complex at Hess Deep (Figs. 4, 7). Some

upper gabbros from Hess Deep are comprised of primitive crystals that have reacted with large amounts of interstitial melt while others are apparently the crystallisation products of evolved melts (e.g., Pedersen et al. 1996; Natland et al. 1996; Hanna 2004; Coogan et al. 2002a). For example, some samples from ODP Hole 894G contain high-anorthite plagioclase, high-chromium clinopyroxene and high-nickel olivine but the bulk compositions of these rocks are evolved. Simple trapped melt calculations, based on the data presented by Hanna (2004) and using the calculation method described in Coogan et al. (2001), suggest typical trapped melt fractions of ~30% in the northern scarp samples (but see earlier discussion of the meaning of these calculations). Based on crystal size distributions there is no evidence that the primitive crystals are xenocrysts suggesting that at least some of the Hole 894 G gabbros crystallised from relatively primitive melts (Coogan et al. 2002a). The evolved bulk compositions simply reflect inefficient removal of interstitial melt from the cumulate. Samples from the northern scarp at Hess Deep apparently do not show evidence for a primitive parental melt but instead crystallised from evolved melts (Natland and Dick 1996; Hanna 2004).

Primitive high-level plutonic rocks from Pito Deep provide evidence that mantle derived melts can be transported to shallow levels within the lower oceanic crust with minimal fractionation occurring along the way. More evolved gabbros from Hess Deep however show that both crystal fractionation, and post-cumulus chemical changes (e.g., trapped liquid shift, metasomatism by an interstitial melt), can generate much more evolved rocks at this structural level. The differences observed between plutonic rocks recovered from Hess Deep and Pito Deep suggest that significant temporal and/or spatial heterogeneities exist in the magma plumbing system beneath the EPR. The crustal thickness, and thus magma supply, along the EPR seems to be relatively constant based on geophysical observations. Additionally, the spreading rates at both the Hess (~135 mm/year) and Pito (~145 mm/year) Deeps are similar. Thus, it seems likely that the differences in magmatic processes observed in the plutonic section either reflect short-term variations in magma supply or variability in the efficiency of hydrothermal heat extraction. The latter process is likely dependent on the location of fault zones to act as high permeability conduits for fluid flow.

Basalts erupted along the EPR provide evidence for temporal and spatial variability in the magma plumbing systems beneath fast-spreading ridges. Basalts sampled along a flow-line away from the EPR, at 10°30′N to 800 kyr suggests that the magma plumbing system goes through periods of erupting more and less fractionated basalts (Batiza et al. 1996; Regelous et al. 1999). In other places the magma system appears relatively constant on this timescale (Batiza et al. 1996). Likewise, in some places basalts erupted at the ends of segments are more fractionated than those at segment centres (e.g., Christie and Sinton 1981; Langmuir et al. 1986).

We hypothesize that the mechanism of lower crustal construction varies along the EPR from a gabbro glacier-like mechanism (Pito Deep), to a hybrid sill and glacier mechanism (Hess Deep). This may be due to more rapid cooling of the lower crust exposed at the Hess Deep than at the Pito Deep. Crystallisation in sills in the deeper crust at Hess Deep would allow the parental melt for many of the upper gabbros to become evolved. Additionally, more rapid cooling of the upper plutonic complex would prevent efficient crystal-melt separation, through compaction, in a crystal mush zone beneath the AMC leading to high ‘‘trapped melt’’ fractions. In other places, such as Pito Deep, compaction of the subsiding crystal mush may efficiently extract the interstitial melt from the cumulates (e.g., Henstock 2002).

A difference in thermal structure may be explained by spatial or temporal heterogeneity. The current EPR axis at the same latitude as Hess Deep has deep bathymetry (>3,000 m) and is made up of many short segments (Lonsdale 1988) suggesting that the entire system may be relatively cool. In contrast, the crustal section studied at Pito Deep was apparently constructed in the mid-point of a segment. Alternatively, or additionally, temporal changes in thermal structure of the crust (e.g., episodic growth of deep faults allowing fluid flow to penetrate the deeper crust) may occur. For example, Lonsdale (1988; his Fig. 18) suggests that when the crust exposed at Hess Deep was accreted there may have been a major discontinuity in the EPR axis affecting crustal accretion. There may even be a positive feedback with cooler crust being faulted more allowing more deep-seated hydrothermal cooling. The spatial and hence temporal scale of crustal accretion heterogeneities is difficult to constrain using the present sample suite from the EPR due to the fact that only two places have been sampled. Once IODP Hole 1256 is deepened further into the gabbros a third dataset will be available for comparison with the lower crust exposed at the Hess and Pito Deeps.

A working model

A model to explain the similarities and differences in the plutonic rocks observed at Pito Deep and Hess Deep based on spatial and/or temporal variability in the processes operating at a fast-spreading ridge is shown in Fig. 11. During times, and/or in places, of robust magma supply, and/or limited deep hydrothermal cooling, the crust beneath the AMC cools too slowly for much crystallisation to

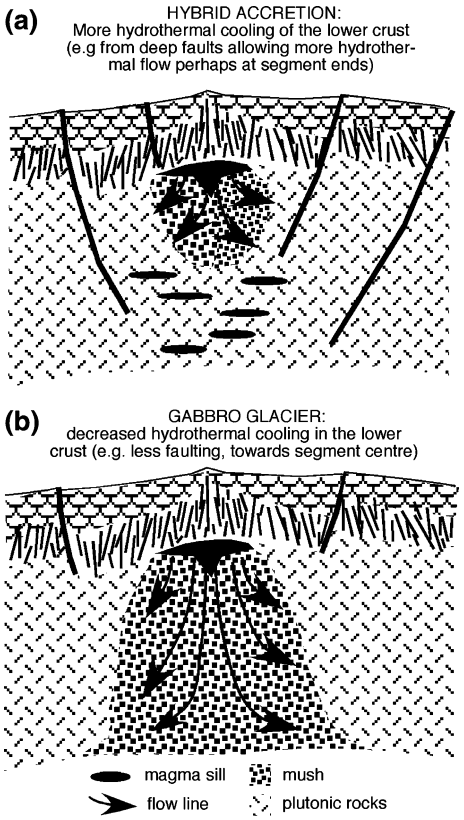

Fig. 11 Model for lower crustal accretion at fast-spreading ridges based on the model of Coogan (2007). **a** Where hydrothermal cooling of the lower crust efficiently removes heat some melt can crystallise in situ as it migrates through the crust. Additionally the mush subsiding from the AMC cools rapidly and freezes-in interstitial melt. This hybrid model may be applicable to Hess Deep. **b** Where the lower crust is cooled less by hydrothermal circulation most crystallization occurs within the AMC and a subsiding mush generates most of the lower crust. This model may be applicable at Pito Deep

occur in situ at this level. Crystallisation mainly occurs within the AMC due to heat loss through its roof. The cumulates formed then subside to form the underlying crust. Vertical, axis-parallel magmatic foliations are generated during subsidence of the crystal mush with interstitial melt acting as a lubricant such that little or no intracrystal deformation is necessary (Quick and Denlinger 1993). Interstitial melt is compacted out of the subsiding mush and driven back towards the AMC (e.g., Henstock 2002) adding to the differentiation of the melt in this body. This compaction efficiently separates crystals and melt producing primitive cumulates. Vertical layering and foliation in the upper gabbros (Fig. 3) may either be transposed into parallelism with the Moho as in the original gabbro glacier models (Nicolas et al. 1988; Quick and Denlinger 1993; Phipps Morgan and Chen 1993; Henstock et al. 1993) or may be unrelated to the foliation and layering in the deeper gabbros. For example, a crystal slurry may subside through the LVZ and spread laterally at depth (e.g., Buck 2000). Either way, the occurrence of layering in the upper gabbros suggests that there may not be any fundamental difference between the mechanism of formation of the upper and lower gabbros as has been suggested based on observations in the Oman ophiolite (MacLeod and Yaouancq 2000).

During periods, and/or in places, of more limited magma supply and/or more extensive deep hydrothermal cooling the lower part of the plutonic section become sufficiently rigid that ascending melt sometimes pools in the lower crust (e.g., in sills). Because the lower crust is relatively cool magmas that pond in sills partially crystallise. Some melt is still delivered to the AMC either directly or having ponded and partially crystallised in the lower crust. Some crystal subsidence is still required on thermal grounds (Coogan et al. 2002b; Maclennan et al. 2004), to explain the occurrence of plutonic rocks that show evidence for assimilation at the roof of the AMC at depths of at least 800 mbsd (Gillis et al. 2003), and to form the vertical magmatic fabrics within the upper plutonic rocks. Melt crystallization in sills in the deeper crust leads to the average lower crustal composition becoming more evolved upwards. This compositional stratification is accentuated because the mush subsiding from the AMC cools rapidly, preventing interstitial melt being efficiently compacted out of the crystal mush. This leads to larger amounts of interstitial melt back-reacting with the cumulus crystals and leads to more evolved bulk rock compositions. The relative importance of crystallization at depth and ''trapped melt'' in making the upper gabbros at Hess Deep evolved is unclear although the latter is certainly an important process (Coogan et al. 2002a; Pedersen et al. 1996).

Acknowledgments Journal reviews from Jean Bédard and an anonymous reviewer are gratefully acknowledged as is Meagan Pollock's generosity in allowing us to use her unpublished data. This study was made possible through the dedication of the captain and crew of the R/V *Atlantis*, the pilots of the *Jason* II and the Pito Deep 2005 Scientific Party. Kerri Heft and Kathy Gillis are thanked for careful sample curation and transport and Nick Haymon is thanked for help with accessing seafloor video imagery. Jody Spence, Gary Dwyer and Rob Wilson are thanked for assistance with ICP-MS, DCP and electron microprobe analyses respectively. Funding for the cruise came from NSF grant OCE-0222154 to JAK and EMK and for the shore-based study from an NSERC discovery grant to LAC and an NSERC Undergraduate Student Research Award to NWP.

References

Anders E, Grevesse N (1989) Abundances of the elements: Meteoric and solar. Geochim Cosmochim Acta 53:197–214

Batiza R, Niu Y, Karsten JL, Boger W, Potts E, Norby L, Butler R (1996) Steady and non-steady magma chambers below the East Pacific Rise. Geophys Res Lett 23(3):221–224

Bédard JH (1991) Cumulate recycling and crustal evolution in the Bay of Islands ophiolite. J Geol 99:225–249

Bédard JH (1994) A procedure for calculating the equilibrium distribution of trace elements amoungst the minerals of cumulate rocks, and the concentration of the trace elements in co-existing liquids. Chem Geol 118:143–153

Boudier F, Nicolas A, Ildefonse B (1996) Magma chambers in the Oman ophiolite: fed from the top and the bottom. Earth Planet Sci Lett 144:239–250

Buck WR (2000) Can flow of dense cumulate through mushy upper gabbros produce lower gabbros at a fast spreading center? In: Dilek Y, Moores E, Elthon D, Nicolas A (eds) Ophiolites and oceanic crust: new insights from field studies and ocean drilling, vol 349. Geological Society of America, pp 121–127

Cande SC, Kent DV (1995) Revised calibration of the geomagnetic polarity timescale for the late Cretaceous and Cenozoic. J Geophys Res 101(B4):6093–6095

Chen YJ (2001) Thermal effects of gabbros accretion from a deeper second melt lens at the fast spreading East Pacific Rise. J Geophys Res 106(B5):8581–8588

Christie DM, Sinton JM (1981) Evolution of abyssal lavas along propagating segments of the Galapagos spreading center. Earth Planet Sci Lett 56:321–335

Constantin M (1999) Gabbroic intrusions and magmatic metasomatism in harzburgites from the Garrett transform fault: implications for the nature of the mantle-crust transition at fast spreading ridges. Contrib Mineral Petrol 136:111–130

Constantin M, Hékinian R, Ackermand D, Stoffers P (1995) Mafic and ultramafic intrusions in upper mantle peridotties from fast spreading centers of the Easter Microplate (South East Pacific). In: Vissers RLM, Nicolas A (eds) Mantle and lower crustal exsposures in Ocean Ridges and in Ophiolites, Kluwer, pp 71–120

Constantin M, Hékinian R, Bideau D, Hébert R (1999) Construction of the oceanic lithosphere by magmatic intrusions: Petrological evidence from plutonic rocks formed along the fast-spreading East Pacific Rise. Geology 24(8):731–734

Coogan LA (2007) The lower oceanic crust. In: Turekian K, Holland HD (eds) Treatise on Geochemistry, Elsevier (in press)

Coogan LA, Kempton PD, Saunders AD, Norry MJ (2000) Evidence from plagioclase and clinopyroxene major and trace element compositions for melt aggregation within the crust beneath the Mid-Atlantic Ridge. Earth Planet Sci Lett 176(2):245–257

Coogan LA, MacLeod CJ, Dick HJB, Edwards SJ, Kvassnes A, Natland JH, Robinson PT, Thompson G, O'Hara MJ (2001) Whole-rock geochemistry of gabbros from the Southwest Indian Ridge: constraints on geochemical fractionations between the upper and lower oceanic crust and magma chamber processes at (very) slow-spreading ridges. Chem Geol 178(1–4):1–22

Coogan LA, Gillis KM, MacLeod CJ, Thompson G, Hékinian R (2002a) Petrology and geochemistry of the lower ocean crust formed at the East Pacific Rise and exposed at Hess Deep: a synthesis and new results. Geochem. Geophys. Geosyst. Special issue: The Oman ophiolite and ocean ridge processes. doi: 10.1029/2001GC000230

Coogan LA, Jenkin GRT, Wilson RN (2002b) Constraining the cooling rate of the lower oceanic crust: a new approach applied to the Oman ophiolite. Earth Planet Sci Lett 199:127–146

Coogan LA, Thompson G, MacLeod CJ (2002c) A textural and geochemical investigation of high level gabbros from the Oman ophiolite: implications for the role of the axial magma chamber at fast spreading ridges. Lithos 63:67–82

Crawford WC, Webb SC (2002) Variation in the distribution of magma in the lower crust and at the Moho beneath the East Pacific Rise at 9°–10°N. Earth Planet Sci Lett 203:117–130

Detrick RS, Buhl P, Vera E, Mutter J, Orcutt J, Madsen J, Brocher T (1987) Multi-channel seismic imaging of a crustal magma chamber along the East Pacific Rise. Nature 326(6108):35–41

Dewey JF, Kidd WSF (1977) Geometry of plate accretion. Geol Soc Am Bull 88:960–968

Dunn RA, Toomey DR, Solomon SC (2000) Three-dimensional seismic structure and physical properties of the crust and shallow mantle beneath the East Pacific Rise at 9°30′N. J Geophys Res 105(B10):23537–23555

Eggins SM, Woodhead JD, Kinsley LPJ, Mortimer GE, Sylvester P, McCoullock MT, Hergt JM, Handler MR (1997) A simple method for the precise determination of > 40 trace elements in geological samples by ICPMS using enriched isotope internal standardisation. Chem Geol 134:311–326

Elthon D, Stewart M, Ross DK (1992) Compositional trends of minerals in oceanic cumulates. J Geophys Res. 979(B11):15189–15199

Francheteau J, Patriat P, Segoufin J, Armijo R, Doucoure M, Yelleschaouche A, Zukin J, Calmant S, Naar DF, Searle RC (1988) Pito and Orongo Fracture-Zones—the Northern and Southern Boundaries of the Easter Microplate (Southeast Pacific). Earth Planet Sci Lett 89(3–4):363–374

Garrido CJ, Kelemen PB, Hirth G (2001) Variation of cooling rate with depth in the lower crust formed at an oceanic spreading ridge: plagioclase crystal size distributions in gabbros from the Oman ophiolite. Geochem Geophys Geosys 2:2000GC000136

Ghiorso MS, Sack RO (1995) Chemical mass transfer in magmatic processes IV. A revised and internally consistent thermodynamic model for the interpolations of liquid-solid equilibria in magmatic systems at elevated temperatures and pressures. Contrib Mineral Petrol 119:197–212

Gillis KM, Mével C, Allan J (1993) Proc. ODP, Init. Repts., vol 147. Ocean Drilling Program, College Station, Texas, p 366

Grove TL, Bryan WB (1983) Fractionation of pyroxene-phyric MORB at low pressure: an experimental study. Contrib Mineral Petrol 84:293–309

Grove TL, Kinzler RJ, Bryan WB (1992) Fractionation of Mid-Ocean Ridge Basalt (MORB). In: Phipps Morgan J, Blackman DK, Sinton JM (eds) Mantle flow and melt generation at Mid-Ocean Ridges, vol 71. American Geophysical Union, pp 281–311

Hanna HD (2004) Geochemical variations in basaltic glasses from an incipient rift and upper level gabbros from Hess Deep, Eastern Equatorial Pacific. MSc. Duke University, Durham, p 94

Hart SR, Dunn T (1993) Experimental cpx/melt partitioning of 24 trace elements. Contrib Mineral Petrol 113:1–8

Heft KL, Gillis KM (2005) Fluid flow and hydrothermal alteration patterns in sheeted Dikes at Pito Deep. EOS Trans AGU, Fall Meeting 86(52):T33D–0583

Hékinian R, Bideau D, Francheteau J, Cheminee JL, Armijo R, Lonsdale P, Blum N (1993) Petrology of the East Pacific Rise Crust and upper mantle exposed in Hess Deep (East Equatorial Pacific). J Geophys Res 98(B5):8069–8094

Hékinian R, Francheteau J, Armijo R, Cogne JP, Constantin M, Girardeau J, Hey R, Naar DF, Searle R (1996) Petrology of the Easter microplate region in the South Pacific. J Volc Geotherm Res 72(3–4):259–289

Henstock TJ (2002) Compaction control of melt distribution at fast-spreading mid-ocean ridges. Geophys Res Lett 29

Henstock TJ, Woods AW, White RS (1993) The accretion of Oceanic Crust by episodic sill intrusion. J Geophys Res 98(B3):4143–4161

Herzberg C (2004) Partial crystallisation of mid-ocean ridge basalts in the crust and mantle. J Petrol 45(12):2389–2405

Hey RN, Johnson PD, Martinez F, Korenaga J, Somers ML, Huggett QJ, Lebas TP, Rusby RI, Naar DF (1995) Plate boundary

reorganization at a large-offset, rapidly propagating rift. Nature 378(6553):167–170
Karson JA (2005) Internal structure of the upper oceanic crust generated at fast to intermediate rates: the view from tectonic windows in the Pacific. In: EOS Trans AGU 86(52), Fall Meet pp T23F-03
Karson JA, Klein EM, Hurst SD, Lee C, Rivizzigno P, Curewitz D, Morris AR, Party HDS (2002) Structure of uppermost fast-spread oceanic crust exposed at the Hess Deep Rift: Implications for subaxial processes at the East Pacific Rise. Geochem Geophys Geosys 3. doi:10.1029/2001GC000155
Kelemen PB, Aharanov E (1998) Periodic formation of magma fractures and generation of layered gabbros in the lower crust beneath oceanic spreading ridges. In: Buck WR, Delaney PT, Karson JA, Lagrabrielle Y (eds) Faulting and Magmatism at Mid-Ocean Ridges, vol 106. American Geophysical Union, Washington, pp 267–289
Kelemen PB, Koga K, Shimizu N (1997) Geochemistry of gabbro sills in the crust-mantle transition zone of the Oman ophiolite: implications for the origin of the oceanic lower crust. Earth Planet Sci Lett 146:475–488
Kent GM, Harding AJ, Orcutt JA (1990) Evidence for a smaller magma chamber beneath the East Pacific Rise at 9°30′N. Nature 344:650
Klein EM, Langmuir CL, Staudigelv H (1991) Geochemistry of basalts from the Southeast Indian Ridge, 115–138°E. J Geophys Res 96:2089–2107
Korenaga J, Kelemen PB (1997) Origin of gabbro sills in the Moho transition zone of the Oman ophiolite: implications for magma transport in the oceanic crust. J Geophys Res 102(B12):27729–27749
Korenaga J, Kelemen PB (1998) Melt migration through the oceanic lower crust: a constraint from melt percolation modelling with finite solid diffusion. Earth Planet Sci Lett 156:1–11
Langmuir CH (1989) Geochemical consequences of in situ differentiation. Nature 340:199–205
Langmuir CH, Bender JF, Batiza R (1986) Petrological and tectonic segmentation of the East Pacific Rise, 5°30′-14°30′N. Nature 322:422–429
Lissenberg CJ, Bedard JH, van Staal CR (2004) The structure and geochemistry of the gabbro zone of the Annieopsquotch ophiolite, Newfoundland: implications for lower crustal accretion at spreading ridges. Earth Planet Sci Lett 229:105–123
Lonsdale P (1988) Structural pattern of the Galapagos microplate and evolution of the Galapagos triple junctions. J Geophys Res 93(B11):13551–13574
Lonsdale PF (1999) Provenance and deformation of the volcanic section exposed at Hess Deep. In: Eos Trans Am Geophys Union, 80(46), Fall Meet Suppl, F994
Maclennan J, Hulme T, Singh SC (2004) Thermal models of oceanic crustal accretion: linking geophysical, geological and petrological observations. Geochem Geophys Geosys 5(2). doi: 10.1029/2003GC000605
MacLeod CJ, Yaouancq G (2000) A fossil melt lens in the Oman ophiolite: Implications for magma chamber processes at fast spreading ridges. Earth Planet Sci Lett 176(3–4):357–373
MacLeod CJ, Boudier F, Yaouancq G, Richter C (1996) Gabbro Fabrics from Site 894, Hess Deep: Implications for magma Chamber processes at the East Pacific Rise. In: Mevel C, Gillis KM, Allan JF, Meyer PS (eds) Proc ODP Sci Res, vol 147. Ocean Drilling Program, College station, Texas, pp 317–328
Martinez F, Naar DF, Reed TB, Hey RN (1991) 3-Dimensional Seamarc Ii, gravity, and magnetics study of large-offset rift propagation at the Pito Rift, Easter Microplate. Mar Geophys Res 13(4):255–285
Meyer PS, Bryan BB (1996) Petrology of basaltic glasses from the TAG segment: implications for a deep hydrothermal heat source. Geophys Res Lett 23(23):3435–3438
Morgan LA, Karson JA, Haymon NW, Varga RJ, Hurst SD (2005) Internal Structure of Basaltic Lavas and Sheeted Dikes in 3 Ma Super-Fast EPR Crust Exposed at Pito Deep. EOS Trans AGU, Fall Meeting 86(52) T33D-0588
Naar DF, Hey RN (1991) Tectonic evolution of the Easter Micorplate. J Geophys Res 96(B5):7961–7993
Naar DF, Martinez F, Hey RN, Reed TB, Stein S (1991) Pito rift: How a large-offset rift propagates. Mar Geophys Res 13(4):287–309
Natland JH, Dick HJB (1996) Melt migration through high-level gabbroic cumulates of the east pacific rise at the Hess Deep: the origin of magma lenses and the deep crustal structure of fast-spreading ridges. In: Mevel C, Gillis KM, Allan JF, Meyer PS (eds) Proceedings of the ODP, Science Results 147, vol 147. Ocean Drilling Program, College Station, Texas, pp 21–58
Nicolas A (1992) Kinematics in magmatic rocks with special reference to gabbros. J Petrol 33(4):891–915
Nicolas A, Boudier F, Ceuleneer G (1988) Mantle flow patterns and magma chambers at ocean ridges: evidence from the Oman ophiolite. Mar Geophys Res 9:293–310
Pedersen RB, Malpas J, Falloon T (1996) Petrology and geochemistry of gabbroic and related rocks from Site 894, Hess Deep. In: Mevel C, Gillis KM, Allan JF, Meyer PS, (eds) Proceedings of the Science Results ODP Leg 147, College station, Texas, pp 3–19
Phipps Morgan J, Chen YJ (1993) The Genesis of oceanic crust: magma injection, hydrothermal cooling, and crustal flow. J Geophys Res 98(B4):6283–6297
Pollock MA, Klein EM, Karson JA (2005) Geochemical variability of Dikes and Lavas exposed in the Pito Deep. In: EOS Trans AGU, Fall Meeting 86(52):T33D-0585
Presnall DC, Hoover JD (1987) High pressure phase equilibrium constraints on the origin of mid-ocean ridge basalt. In: Mysen BO (ed) Magmatic processes: physicochemical principles, vol 1. The Geochemical Society, pp 75–90
Quick JE, Denlinger RP (1993) Ductile deformation and the origin of layered gabbro in ophiolites. J Geophys Res 98(B8):14015–14027
Regelous M, Niu Y, Wendt JI, Batiza R, Greig A, Collerson KD (1999) Variations in the geochemistry of magmatism on the East Pacific Rise at 10°30′N since 800 ka. Earth Planet Sci Lett 168:45–63
Reuber I (1990) Diapiric magma intrusions in the plutonic sequence of the Oman ophiolite traced by the geometry and flow patterns of the cumulates. In: Symposium on Diapirism with special reference to Iran, Teheran, pp 315–338
Searle RC, Rusby RI, Engeln J, Hey RN, Zukin J, Hunter PM, Lebas TP, Hoffman HJ, Livermore R (1989) Comprehensive sonar imaging of the Easter Microplate. Nature 341(6244):701–705
Sleep NH (1975) Formation of oceanic crust: some thermal constraints. J Geophys Res 80:4037–4042
Stoffers P, Hékinian R, (1989) Cruise Report SONNE 65 - Midplate II, Hotspot volcanism in the central Southpacific. Berichte - Reports no. 40:126
Stoffers P, Hékinian R, (1992) Cruise Report SONNE 80a - Midplate III, Oceanic volcanism in the Southpacific. Berichte - Reports no. 58:128
Tormey DR, Grove TL, Bryan WB (1987) Experimental petrology of N-MORB near the Kane Fracture Zone: 22–25°N, mid-Atlantic ridge. Contrib Mineral Petrol 96:121–139
Van Orman JA, Grove TL, Shimizu N (2001) Rare earth element diffusion in diopside: influence of temperature, pressure, and ionic radius and an elastic model for diffusion in silicates. Contrib Mineral Petrol 141:687–703